

Impact of Coating Type on the Radiation Response of Germanosilicate Optical Fibers at High Temperatures

H. Boiron, G. Mélin, A. Morana, *Member, IEEE*, D. Lambert, A. Steib, R. Pouyet, L. Kervella, A. Monteville, P. Guitton, S. Chaton, P. Paillet, *IEEE fellow*, T. Robin, and S. Girard, *Senior Member, IEEE*

Abstract—We investigate the combined temperature (30°C and 300°C) and radiation effects (up to 55 kGy of X-rays) on germanosilicate optical fibers with different types of coatings. Dose deposition simulation tools are also used to make a proper comparison.

Index Terms—Aluminum coating, polyimide coating, optical fiber, radiation induced attenuation, hydrogen diffusion

I. INTRODUCTION

In many respects, extreme environments require instrumentation posing a significant scientific challenge. Among these extreme environments, we encounter extreme temperatures (both hot and cold) and radiation-rich environments. Developing instrumentation or systems able to operate in such environments is a challenge in itself. When facing an environment that combines both constraints, only a few viable technological solutions remain.

For several decades, optical fibers have emerged as a very promising technology for such instrumentation. Their compact size, insensitivity to electromagnetic disturbances, relatively low cost, and the ability to efficiently perform distributed measurements over long distances are key advantages offered by fiber-based solutions [1]. Notably, among optical fiber sensors, examples include sensors for strain [2], temperature [3], and radiation [4], each providing solutions for point or distributed measurements [5].

For using an optical fiber solution in such environments, it becomes imperative to carefully select both its chemical composition and its protective coating. Indeed, it is well known that the radiation tolerance, characterized by the Radiation-Induced Attenuation (RIA), of optical fibers is significantly influenced by the nature of dopants and impurities present in the core and cladding [4]. These dopants are also employed to modulate the silica refractive index and build the refractive index profile that defines the light guidance properties and bandwidth. The coating is, firstly, chosen to assure the mechanical resistance of the fiber according to the experienced

environment (radiation, temperature, etc ...) [6] but can also influence the RIA levels. Its associated fiber drawing conditions (speed, tension, etc.) can, indeed, affect the RIA but as we will see later in the abstract, the coating can alter the dose deposition mechanisms in the silica core and then affect the radiation tolerance of the fiber. A conventional acrylate coating can be used for temperature up to 85°C for a long term. However, to withstand temperatures exceeding 300°C, it is mandatory to use either polyimide coatings or metallic coatings such as aluminum or copper.

As part of the 3F2E project, Exail and Photonics Bretagne produced aluminum-coated optical fibers. With the aim of assessing the radiation resistance at high temperatures of these Al-coated fibers, tests were conducted at the LabH6 (a joint laboratory between Exail and the Hubert Curien Laboratory at Jean Monnet University in Saint-Étienne) using the LABHX X-ray machine. To highlight the coating influence, the radiation responses of two other fibers with an identical chemical composition but with acrylate or polyimide coatings were also compared. This abstract focuses on the comparison between the fibers having polyimide or aluminum coating.

In addition to the radiation tests, we also studied the influence of the aluminum coating on dose deposition by photons of various energies within the fiber core with GEANT4 simulation [7]. Indeed, the thin metal layer acts as a shielding material against the most low-energy X-rays. Following the introduction of the experimental setup, we present the initial characterization measurements of the radiation resistance of the germanium-doped multimode graded-index (MMGI) optical fiber at both 30 °C and 300 °C, subjected to a total ionization dose of 55 kGy at a dose rate of 1.53 Gy(SiO₂)/s of X-rays. The impact of temperature and coating type on fiber radiation-induced attenuation (RIA) will be discussed. Lastly, we will conclude by addressing the ongoing and future directions within the scope of this study.

This work was supported by the 3F2E project for “French Fiber Field for Extreme Environment”, funded by the post-pandemic France Economic Stimulus Plan “Relaunch France” aimed at supporting investments and reinforcing the capabilities of the French nuclear industry.

H. Boiron, G. Mélin, A. Steib, L. Kervella, P. Guitton, S. Chaton and T. Robin are with Exail, 22300 Lannion, France. (e-mail: hugo.boiron@exail.com).

A. Morana, and S. Girard are with Laboratoire Hubert Curien, Université Jean Monnet, 42000 Saint-Étienne, France (e-mail: [\[etienne.fr\]\(http://etienne.fr\)\). S. Girard is also with Institut Universitaire de France \(IUF\), Paris, France](mailto:sylvain.girard@univ-st-</p>
</div>
<div data-bbox=)

R. Pouyet and A. Monteville are with Photonics Bretagne, 22300 Lannion, France (e-mail: rpouyet@photonics-bretagne.com).

D. Lambert is with CEA, DAM, DIF, 91297 Arpajon, France (e-mail: damien.lambert@cea.fr).

II. MATERIAL AND METHOD

In this section, we will first describe the opto-geometric characteristics of the different tested optical fibers. Subsequently, we will discuss the impact of the aluminum coating on the dose deposition within the fiber core for photons of varying energy. Finally, we will present our experimental procedure for the radiation tests.

A. Aluminum and polyimide coated fibers

The tested optical fibers are Ge-doped MMGI with the refractive index profiles presented in Fig. 1. The two samples are drawn from two different preforms, manufactured following the same process. The fiber has a core diameter of $50 \mu\text{m}$ and a numerical aperture of 0.20, while its cladding diameter is of $125 \mu\text{m}$. It can be considered that the cores and claddings are identical in the aluminum-coated and polyimide-coated fibers. The polyimide coating has a thickness of $15 \pm 1 \mu\text{m}$ with a density of 1.4 g/cm^3 , whereas the aluminum one has a thickness of $21 \pm 3 \mu\text{m}$ with a density of 2.7 g/cm^3 .

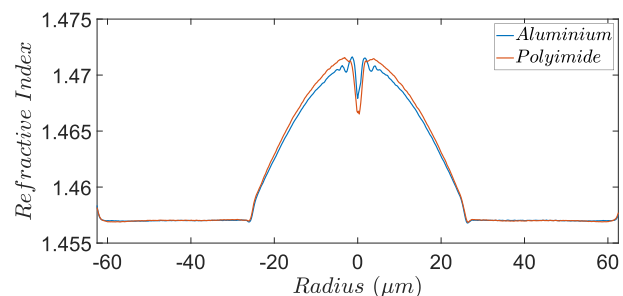


Fig. 1. Refractive index profiles of the two tested optical fibers.

Ge-doped fibers are known for their acceptable radiation tolerance for applications associated with moderate dose levels and involving short fiber lengths, which motivated the selection of this dopant [4]. Additionally, this fiber represents the initial iteration while alternative doping techniques will be further investigated for more radiation-hardened optical fibers.

B. Dose deposition simulation

Initially, it is crucial to examine the impact of the metallic coating on the dose deposition (total ionizing dose, TID) within the fiber core. Indeed, one can anticipate that this coating may partially filter out lower-energy particles of the X-rays beam used for this work. To determine the dose distribution within the irradiated optical fiber (OF) core, we conducted a simulation using Geant4 toolkit [7], [8]. In this study, Geant4 v10.07. patch 4 (released in December 2022) version was employed, alongside with the `em_standard_opt4` physics package. The calculation provides us the dose/fluence ratio for the photons at different energies illustrated in the right y-axis of Fig. 2 for the aluminium-coated fiber, the polyimide-coated fiber and for a germano-silicate bulk. Additional XCOM simulation at the equilibrium allows highlighting the fiber geometry impact on the dose deposition. The comprehensive description of the simulation method is provided in [9], [10]. The energy spectrum used for calculating the deposited dose is the one of the X-ray facility LABHX at the Laboratoire Hubert Curien, operated at 100 kV, as described in [9], simulated by SpekPy [11] and shown in the left y-axis of Fig. 2. From these two simulations, the deposited dose in the core can be

calculated by multiplying the differential fluence spectrum obtained through SpekPy with the dose on fluence, and then integrating the result across the entire energy range emitted by the LABHX.

Simulations show that the aluminum coating reduces the deposited dose in the fiber core by $\sim 13\%$ compared to the polyimide-coated fiber in our irradiation conditions. This difference is considered when adjusting the current, and so the X-ray flux, to ensure a fair comparison between the responses of the two fibers to the TID.

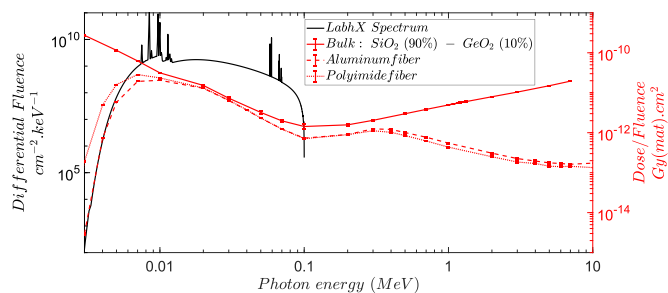


Fig. 2. Left: differential fluence emitted by the LABHX at 100 kV [9] in function of the photon energy. Right: dose over fluence simulation results for the aluminum coated fiber (dashed line), the polyimide coated one (dotted line) and for a germano-silicate bulk (solid line).

It is worth noting that for the energy range from 20 keV to 100 keV the dose deposition between fiber and bulk is almost identical which means that we are at the electronic equilibrium. It is not the case for higher energy. Interestingly, it should be noted from this simulation that for γ -rays with energy higher than 0.5 MeV , aluminum coating seems to enhance by 20% the dose deposition in comparison with polyimide coated fiber.

C. Experimental setup

A white light source (DH 2000 BAL) was employed and an optical spectrum analyzer (OSA, YOKOGAWA AQ6370C) served as the detector as illustrated in Fig. 3. The polyimide version of the developed MMGI was used as both the input and output transport fiber to minimize losses at the junctions and enhance repeatability. The transport fibers were shielded and, therefore, not subjected to irradiation.

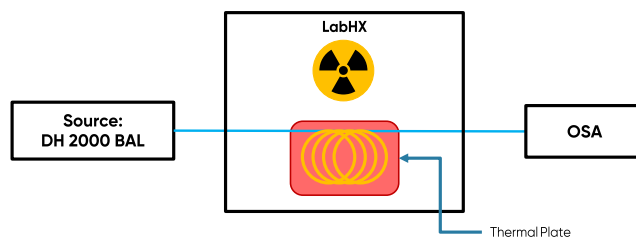


Fig. 3. Experimental setup with a white light as a source and an optical spectrum analyzer (OSA) as a detector.

To ensure sample homogeneity, the fiber was wound in a mono layer coil with an inner diameter of 6.5 cm and an outer diameter of 11.5 cm , as shown in Fig. 4. The spatial homogeneity of the radiation flux across the entire sample is verified by measuring the dose rate at four cardinal points on the coil with an ionization chamber. An inhomogeneity of less than 5% was measured. The single-layer coil is then placed on thermal plate which temperature is set to either 30°C

(considered as room temperature, RT) or 300 °C, and thermal stability is ensured for at least 1 hour before starting irradiation.

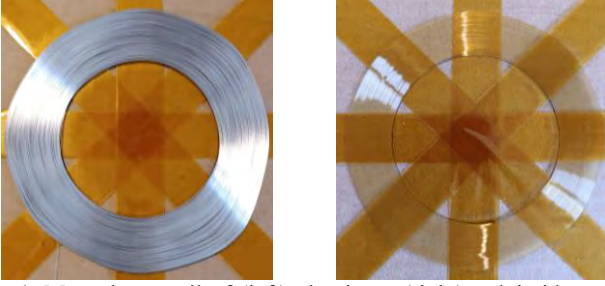


Fig. 4. Mono-layer coil of (left) aluminum (right) polyimide-coated optical fibers.

The dose rate was set at 1.53 Gy(SiO₂)/s. As demonstrated in the previous section, the dose deposited in the fiber core will not be exactly the same for aluminum and polyimide-coated fibers under identical irradiation conditions. To facilitate a meaningful comparison of results, it is necessary to ensure an equal deposited dose in both cases. To achieve this, the irradiator current will be increased by 10 % during tests on the aluminum-coated fiber in order not to change the dose rate between the two tests.

III. PROCESSING AND RESULTS

This section presents the experimental study concerning irradiation at 30 °C and 300 °C with a dose rate of 1.53 Gy/s, up to a total deposited dose of 25 – 55 kGy, for both polyimide and aluminum-coated fibers.

A. From the transmission spectrum to the spectral RIA measurement

The Optical Spectrum Analyzer (OSA) records the power transmitted ($P(\text{dose}, \lambda)$) by the source throughout the experiment at 50 s intervals, with a spatial resolution set to 1 nm between 900 nm and 1650 nm. It is essential to distinguish between the transmitted power spectrum and the fiber transmission spectrum. The spectrum measured by the OSA is dependent on the emission spectrum of the used white light source. Fig. 5 illustrates the transmitted power spectrum before irradiation (i.e., at 0 kGy) and at the conclusion of irradiation (i.e., at 55 kGy) for both fibers at $T = 300$ °C.

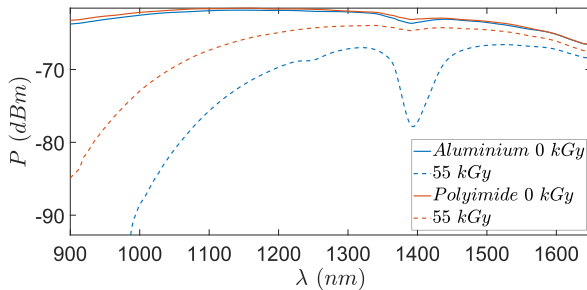


Fig. 5. Transmitted power spectrum before irradiation (i.e., at 0 kGy) and at the conclusion of irradiation (i.e., at 55 kGy) for aluminum (in blue) and polyimide (in orange) coated fibers at $T = 300$ °C.

Fig. 5 indicates that the transmitted power by both fibers is relatively identical. It is noteworthy that the source remains consistent across both experiments, with only the splices with

the transport fibers being remade between experiments to reduce experimental uncertainties. Subsequently, we observe distinct differences in the spectra at the end of irradiation, revealing an overall higher radiation sensitivity of the aluminum-coated fiber compared to the polyimide-coated one.

B. Coating influence on the RIA

This sensitivity is expressed through the measurement the RIA expressed in dB/km, calculated using the equation:

$$RIA(D, \lambda) = - \frac{P(D, \lambda) - P(D = 0, \lambda)}{L} \quad (1)$$

with L the sample length expressed in km, D the deposited dose and λ the considered wavelength. Fig. 6 compares the RIA spectra for both fibers after a TID of 25 kGy at 30 °C and 300 °C.

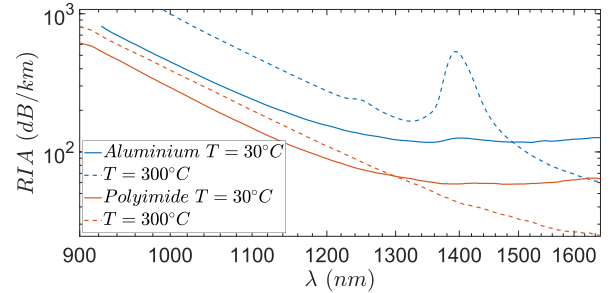


Fig. 6. RIA spectra for aluminum (blue) and polyimide (orange) coated fibers after a TID of 25 kGy (@ 1.53 Gy/s) at two different temperatures of irradiation: 30 °C (solid lines) and 300 °C (dashed lines).

Fig. 6 illustrates that the trend of RIA increases exponentially (linearly in log scale) with decreasing wavelength across the spectral range from 900 nm to 1650 nm. As discussed in the literature, the known defects responsible for RIA in this wavelength range for germanium-doped fibers are GeX and GeY centers, having their absorption bands respectively centered respectively at ~ 2.6 eV and ~ 1.38 eV, with full-widths at half-maximum (FWHM) of ~ 0.97 eV and ~ 0.71 eV [4], [12]. Some not-yet identified defects are also probably contributing. From Fig. 6, it is evident that at both temperatures, the aluminum-coated fiber exhibits higher RIA compared to the polyimide-coated one, as initially indicated in Fig. 5. However, for the polyimide-coated fiber, albeit still observable in the other fiber, losses at longer wavelengths (above 1500 nm) decrease at higher temperatures. Indeed, a distinct absorption band disappears at 300 °C, according to its spectral position it may be associated to the defects today known as Ge-STH band [4]. Studies involving deconvolution of defect absorption bands will be presented in the final paper to gain a deeper understanding of this phenomenon.

A somewhat unexpected result, as demonstrated in Fig. 6, is that the RIA is stronger at 300 °C than at 30 °C. Contrary to the well-known thermal bleaching, in this case, the temperature accentuates the losses. However, this effect has been previously observed in germanium-doped multimode step index (MMSI) fibers [12]. Simulations studying the effects of temperature on light propagation within the fiber are currently underway to see how such effect could concur to the temperature dependence of RIA. Additionally, measurements of the temperature-

dependent variation of intrinsic losses in the fiber are also being conducted.

Finally, another notable effect observed in the results presented in Fig. 6 is the appearance of two absorption peaks at 1240 nm and 1390 nm in the RIA at 300 °C for the aluminum-coated fiber. These peaks indicate the trapping of hydrogen within the fiber matrix to form Si-OH and Ge-OH bonds, with absorption peaks centered at 1390 nm and 1408 nm, respectively. The absorption peak at 1240 nm is attributed to Si(Ge)-OH bonds but also possibly to the presence of molecular hydrogen in the silica based glass matrix [13]. At high temperatures, hydrogen diffuses into the fiber and readily binds to the irradiated matrix by interacting and passivating dangling bonds either created during the drawing or by irradiation. Further studies have shown that hydrogen fixation in the matrix occurs solely through thermal treatment at 300°C without irradiation, albeit at a slower rate and in lesser quantities. This will be elaborated upon in the final paper of this study, but could be explained by a larger concentration of X-NBOHCs (X=Si or Ge) in the irradiated samples. The interaction of hydrogen with NBOHC lead to the appearance of the X-OH absorption peaks:

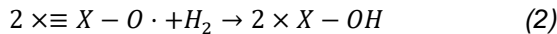


Fig. 7 depicts the kinetics of RIA for both fibers as a function of time and dose at the wavelengths of 1064 nm and 1310 nm, as well as at the absorption peak wavelength of 1390 nm at $T = 300$ °C. The dashed line indicates the stop of irradiation after a TID of 55 kGy (@1.53 Gy/s). The red zone corresponds to recovery at 300 °C.

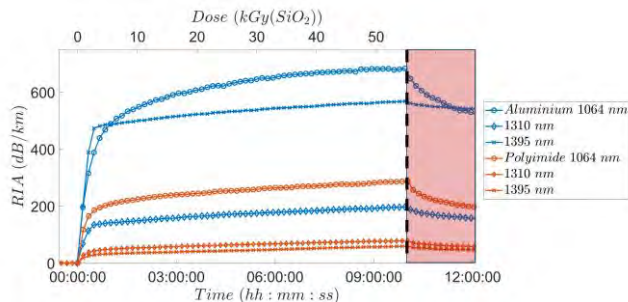


Fig. 7. Evolution of RIA for both fibers as a function of time and dose at 1064 nm and 1310 nm, as well as at the absorption peak wavelength of 1390 nm at $T=300$ °C. The dashed line indicates the stop of irradiation after a total dose of 55 kGy (@1.53 Gy/s). The red zone corresponds to recovery at 300 °C.

As explained earlier, the RIA increases rapidly in the first few kGy then slowly until 55 kGy, and it can indeed be considered that 90% of the final RIA is reached after a dose of 25 kGy. Fig. 7 notably demonstrates the rapid growth and saturation of RIA at 1390 nm caused by hydrogen diffusion in the case of the aluminum-coated fiber. Additionally, Fig. 7 illustrates the recovery phase at 300 °C (red rectangle). A rapid recovery at 300°C indicates that the defects created by radiation are unstable at this temperature and partially recombine.

IV. CONCLUSION & PERSPECTIVES

In this abstract, we investigated the behaviour of germanium-doped MMGI optical fibers irradiated at room temperature and high temperature (300 °C). The high thermal constraint

necessitates the use of special coatings such as polyimide and aluminum. Initially, a GEANT4 simulation was conducted to calculate the relative shielding of the aluminum coating compared to polyimide, enabling coherent comparative tests under X-rays. Subsequently, RIA spectra at 30 °C and 300 °C up to 55 kGy (@1.53 Gy/s) were measured for both fibers between 900 and 1650 nm. On the contrary to what it is commonly expected, we found that the RIA increases when the temperature increases from 30°C to 300°C. Furthermore, absorption peaks related to hydrogen diffusion toward the core in the case of hermetic aluminum coated fibers are observed.

Additional experiments have been conducted or are underway to further understand the mentioned phenomena. We have already investigated the influence of temperature on the fiber intrinsic losses and hydrogen diffusion, as well as the impact of dose rate. Next, simulations will be conducted on the temperature influence on guiding effects within the fiber, and we will test the same fiber with an acrylate coating.

REFERENCES

- [1] B. Lee, « Review of the present status of optical fiber sensors », *Opt. Fiber Technol.*, vol. 9, n° 2, p. 57-79, avr. 2003, doi: 10.1016/S1068-5200(02)00527-8.
- [2] H. Di *et al.*, « Review of optical fiber sensors for deformation measurement », *Optik*, vol. 168, p. 703-713, sept. 2018, doi: 10.1016/j.ijleo.2018.04.131.
- [3] E. Schena *et al.*, « Fiber Optic Sensors for Temperature Monitoring during Thermal Treatments: An Overview », *Sensors*, vol. 16, n° 7, p. 1144, juill. 2016, doi: 10.3390/s16071144.
- [4] S. Girard *et al.*, « Overview of radiation induced point defects in silica-based optical fibers », *Rev. Phys.*, vol. 4, p. 100032, nov. 2019, doi: 10.1016/j.revip.2019.100032.
- [5] P. Lu *et al.*, « Distributed optical fiber sensing: Review and perspective », *Appl. Phys. Rev.*, vol. 6, n° 4, p. 041302, déc. 2019, doi: 10.1063/1.5113955.
- [6] G. Mélin *et al.*, « Radiation Resistant Single-Mode Fiber with Different Coatings for Sensing in High Dose Environments », *IEEE Trans. Nucl. Sci.*, vol. 66, n° 7, p. 1657-1662, juill. 2019, doi: 10.1109/TNS.2018.2885820.
- [7] S. Agostinelli *et al.*, « Geant4—a simulation toolkit », *Nucl. Instrum. Methods Phys. Res. Sect. Accel. Spectrometers Detect. Assoc. Equip.*, vol. 506, n° 3, p. 250-303, juill. 2003, doi: 10.1016/S0168-9002(03)01368-8.
- [8] J. Allison *et al.*, « Recent developments in Geant4 », *Nucl. Instrum. Methods Phys. Res. Sect. Accel. Spectrometers Detect. Assoc. Equip.*, vol. 835, p. 186-225, nov. 2016, doi: 10.1016/j.nima.2016.06.125.
- [9] A. Meyer *et al.*, « Simulation and Optimization of Optical Fiber Irradiation with X-rays at Different Energies », *Radiation*, vol. 3, n° 1, p. 58-74, mars 2023, doi: 10.3390/radiation3010006.
- [10] D. Lambert *et al.*, « Simulation-assisted Methodology for the Design of Fiber-based Dosimeters for a Variety of Radiation Environments », *IEEE Trans. Nucl. Sci.*, p. 1-1, 2024, doi: 10.1109/TNS.2024.3380318.
- [11] R. Bujila *et al.*, « A validation of SpekPy: A software toolkit for modelling X-ray tube spectra », *Phys. Med.*, vol. 75, p. 44-54, juill. 2020, doi: 10.1016/j.ejmp.2020.04.026.
- [12] C. Campanella, « Combined effects of radiation and temperature on silica-based optical fibers », PhD thesis, University of Saint-Etienne, 2022.
- [13] V. V. Voloshin *et al.*, « Effect of metal coating on the optical losses in heated optical fibers », *Tech. Phys. Lett.*, vol. 35, n° 4, p. 365-367, avr. 2009, doi: 10.1134/S1063785009040233.